



Istanbul Bridge Conference
August 11-13, 2014
Istanbul, Turkey

SEISMIC PERFORMANCE OF AN INNOVATIVE CONCRETE FILLED STEEL TUBULAR TRUSS BRIDGE

Yufan Huang¹, Bruno Briseghella², Tobia Zordan³, Qingxiong Wu²,
Baochun Chen²

ABSTRACT

Ganhaizi Bridge is one of the most unusual viaducts that has been built in China in last years. It has a total length of 1811m, and the innovative structural typology is characterized by concrete filled steel tube (CFST) truss girders and CFST lattice piers. Ganhaizi Bridge is located in a very high intensity seismic area of Sichuan Province, and the structural typology adopted is expected to show a good seismic performance. This paper describes a study on the seismic performance of Ganhaizi Bridge. A multi-point shaking table test on a 1:8 scale specimen with two spans and three lattice high piers was designed and performed. The finite element simulation using OpenSees platform was developed. Results indicate that the frequency and displacement between specimen and prototype correspond to similitude relationship. Finite element analysis results are satisfied with experimental data. Furthermore, the influence of different ground motions are discussed. The bridge remains in elastic stage under strong ground motions, conforming that this innovative lightweight bridge has a favorable seismic performance.

¹PhD Candidate, Department of Construction, Università IUAV di Venezia, 30123 Venice, Italy

²Professor, College of Civil Engineering, Fuzhou University, 350108 Fuzhou, China

³Professor, SIBERC Research Center, Fuzhou University, 350108 Fuzhou, China

Seismic Performance of an Innovative Concrete Filled Steel Tubular Truss Bridge

Yufan Huang¹, Bruno Briseghella², Tobia Zordan³, Qingxiong Wu², Baochun Chen²

ABSTRACT

Ganhaizi Bridge is one of the most unusual viaducts that has been built in China in last years. It has a total length of 1811m, and the innovative structural typology is characterized by concrete filled steel tube (CFST) truss girders and CFST lattice piers. Ganhaizi Bridge is located in a very high intensity seismic area of Sichuan Province, and the structural typology adopted is expected to show a good seismic performance. This paper describes a study on the seismic performance of Ganhaizi Bridge. A multi-point shaking table test on a 1:8 scale specimen with two spans and three lattice high piers was designed and performed. The finite element simulation using OpenSees platform was developed. Results indicate that the frequency and displacement between specimen and prototype correspond to similitude relationship. Finite element analysis results are satisfied with experimental data. Furthermore, the influence of different ground motions are discussed. The bridge remains in elastic stage under strong ground motions, conforming that this innovative lightweight bridge has a favorable seismic performance.

Introduction

When a continuous girder bridge is located in the high mountains and deep valleys, reinforced concrete thin-wall hollow pier is generally adopted for the substructure. Especially the bridge with large-span and high-pier, reasonable light-duty pier shape is considered to reduce for promoting the seismic performance of the whole bridge. During recent construction activity in China, a new exploration in the bridge selection is concrete filled steel tubular (CFST) truss typology, comprises of CFST composite truss girders and lattice piers. With the favorable ductility of CFST materials and lightweight truss structure, the earthquake resistant properties of high pier bridge is expected to achieve. The object of research in this paper is Ganhaizi Bridge, located in a very high intensity seismic region (Sichuan Province, China), one of the most unusual viaducts that have been built in 2012. It has a total length of 1811m, and the innovative structural typology is characterized by adopting steel tubes for nearly entire structure. Fig.1 shows the elevation of the longest multi-span units (from piers No.11 to No.30). The piers are generally composed of four CFST columns connected together by circular steel truss tubes. For the height taller than 90m (No.16-25 pier), at the bottom region of 30m pier height, longitudinal connecting steel tubes are replaced with 40mm thickness of RC webs, to enhance pier stiffness. Slant supports are

¹PhD Candidate, Department of Construction, Università IUAV di Venezia, 30123 Venice, Italy

²Professor, College of Civil Engineering, Fuzhou University, 350108 Fuzhou, China

³Professor, SIBERC Research Center, Fuzhou University, 350108 Fuzhou, China

added on the top of CFST columns and fixed with girder together. Superstructure comprises of concrete bridge deck, steel truss webs and CFST bottom chords. In this paper, a shaking table test is described firstly, then a finite element analysis is developed through OpenSees (Open System for Earthquake Engineering Simulation) [1], comparing test data and numerical results. Finally, the influence of different ground motions are discussed.

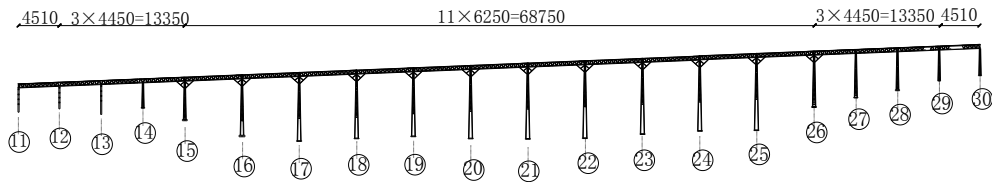


Fig. 1: Elevation of the Ganhaizi Bridge (Unit: cm)

Shaking table test

Based on the high pier zone of real bridge as prototype, a shaking table test with two span and three piers was designed and operated in Fuzhou University. Subjected to the restrictions of length and the bearing capacity of test device, the geometry scale ratio was determined as 1:8, and the highest No. 20 pier is chosen for the pier prototype. Similar materials to the prototype were adopted for manufacture. The specimen height was 13.9m with total mass 20.9t. Elevation drawing and panorama of specimen are presented in Fig. 2 and Fig. 3, respectively. Consider the safety during testing and the difficulty of fixing mass on the circular steel tubes, extra mass is not attached. Table 1 lists the similitude relation of physical quantities according to the dynamic similitude theory [2]. Specimen and countertops were instrumented with accelerometers, displacement transducers and strain gages. Displacement transducers were installed at the top of deck and columns where the maximum displacement is predicted. High-speed camera was adopted to measure displacements. Since stress concentration were expected at the columns where structural stiffness changes, strain gages were mainly installed at the bottom of column, as well as connecting slant support and RC web.

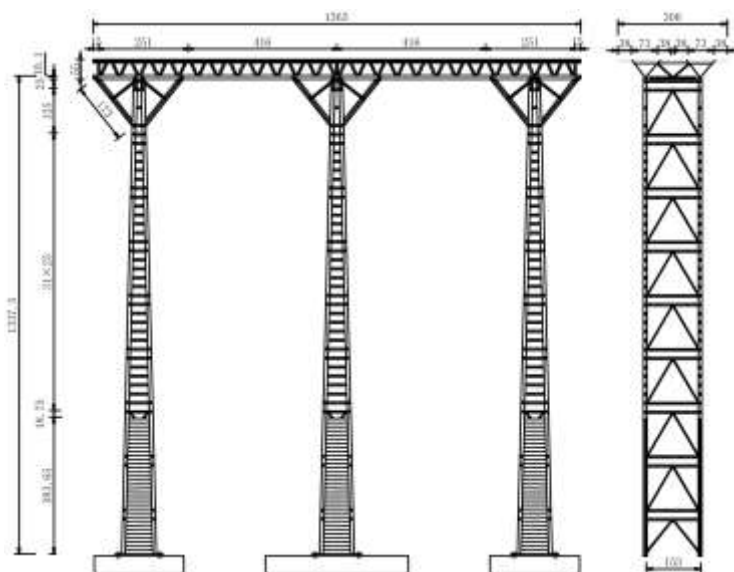


Figure 2. Elevation drawing of the bridge model (unit: cm).



Figure 3. Panorama.

Due to lack of seismic waves at the bridge site, seismic excitation has been carried out by artificial waves based on JTG/T B02-01-2008 [3] and generated according to the design response spectrum. The design seismic acceleration action was 0.362g associated with a reference probability of exceedance, $P_{NCR}=10\%$ in 50 years. Then artificial seismic excitations can be fitted from design spectrum, as shown in Fig. 4 (a), the peak ground acceleration (PGA) was 0.16g. The same waveform and amplitude were adopted for testing, only duration was compressed to 1/8, seen in Fig. 4 (b). Fig. 5 presents response spectrum of input seismic excitations. Dash lines are the fundamental period of prototype and specimen by FEM calculation, both are corresponding to the design spectrum and the PGA are also in accordance.

Table 1. Similitude relation of quantities.

Quantity	Dimension	Scaling law	Scale factors	
			No mass (For specimen test)	Full mass (For FEM analysis)
Linear Length	S_l	$[L]$	$S_l = 1/8$	$S_l = 1/8$
Displacement	S_l	$[L]$	$S_l = S_a S_t^2 = 1/64$	$S_l = S_a S_t^2 = 1/8$
Elastic modulus	S_E	$[E]$	$S_E = 1$	$S_E = 1$
Vertical Strain	S_ε	—	$S_\varepsilon = 1/8$	$S_\varepsilon = 1$
Density	S_ρ	$[\rho]$	$S_\rho = 1$	$S_\rho = 8$
Acceleration	S_a	$[E\rho^{-1}L^{-1}]$	$S_a = 1$	$S_a = 1$
Frequency	S_ω	$[E^{0.5}\rho^{-0.5}L^{-1}]$	$S_\omega = \sqrt{S_E/S_\rho}/S_l = 8$	$S_\omega = \sqrt{S_E/S_\rho}/S_l = \sqrt{8}$
Time	S_T	$[E^{-0.5}\rho^{0.5}L]$	$S_T = 1/S_\omega = 1/8$	$S_T = 1/S_\omega = 1/\sqrt{8}$

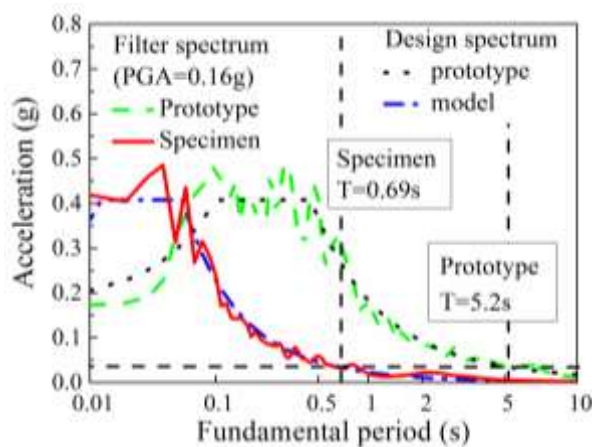
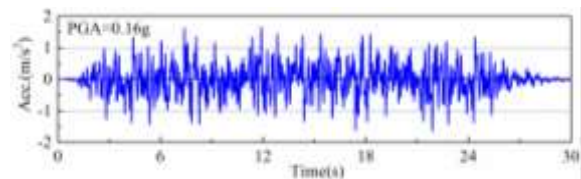
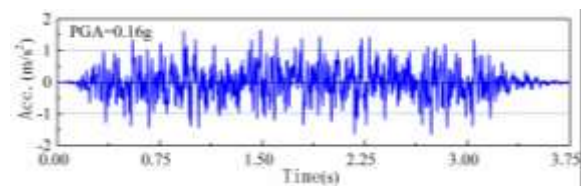


Figure 4. Response spectrum.



(a) Adopted for prototype



(b) Adopted for specimen

Figure 5. Seismic excitations.

$E = 206\text{GPa}$, while remaining parameters were determined by OpenSees manual. The values for concrete compressive properties were obtained from material tests. The loading and unloading rules used in the FEM were calculated based on concrete02 model. Fig. 8 shows the general stress-strain curves for both unconfined and confined concrete. The pre-peak region of compressive stress-strain curve for the confined concrete is modeled using the equations suggested by Mander et al. [6], and confining pressure models are proposed using the equations suggested by Liang and Fragomeni [7], which account for the effects of material properties and column geometry.

A Rayleigh type viscous damping, proportional to mass and initial stiffness was adopted for the first two models with coefficients determined by selecting a damping ratio of 2%. The incremental equations of motion were integrated with Newmark's method ($\beta = 0.25$, $\gamma=0.5$). Newton-Raphson's iteration method was used to enforce equilibrium at each time step. Moreover, for all models, gravity loads were applied first, then followed by the dynamic analysis. For full mass model, according to similitude relationship, 8 times node mass was added at each node, and duration of seismic wave was adjusted, which can be implemented conveniently in OpenSees.

Analytical versus experimental results

The accuracy of the modeling approaches is evaluated through comparisons of fundamental frequency, time histories of displacement and strain envelope along columns. After white noise excitation, fundamental frequency of specimen is identified through power spectral by fast Fourier transform (FFT). Dynamic characteristics of prototype (real bridge) is evaluated for comparison. FEM of the whole bridge was built by the FE software Midas/Civil 2010, which is not mentioned here due to the space limitation. Numerical results of frequency are shown in Table 2. It can be seen that frequency ratio is 1:7.47 in the first order natural frequency and 1:7.66 in the second order, close to the theoretical frequency ratio of 1:8. Table 3 shows frequency comparison between prototype and full mass model. Results indicate that frequency ratio is 1:2.71 in the first order natural frequency and 1:2.93 in the second order, close to the theoretical frequency ratio of 1:2.828. Hence, fundamental frequency comparison demonstrates the accuracy of theoretical similitude relationship, illustrates the dynamic characteristics of specimen can reflect to the real bridge.

Table 2. Fundamental frequency comparison between real bridge and specimen.

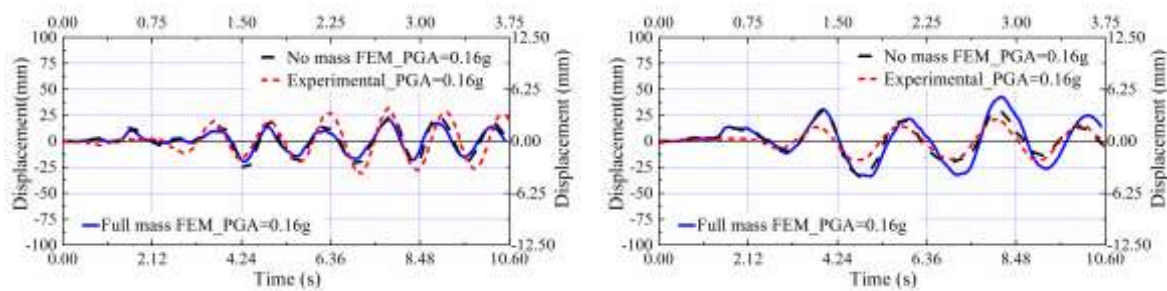
Order	(1) Real bridge	(2) Specimen	(2):(1)	Theoretical value	Error
1	0.194 Hz	1.45 Hz	1:7.47	1:8	6.63%
2	0.274 Hz	2.10 Hz	1:7.66	1:8	4.25%

Table 3. Fundamental frequency comparison between real bridge and full mass model.

Order	(1) Real bridge	(3) Full mass FEM	(3): (1)	Theoretical value	Error
1	0.194 Hz	0.526 Hz	1:2.71	1:2.828	4.10%
2	0.274 Hz	0.803 Hz	1:2.93	1:2.828	3.64%

Time histories of displacement on the top of center columns offers insight into response of

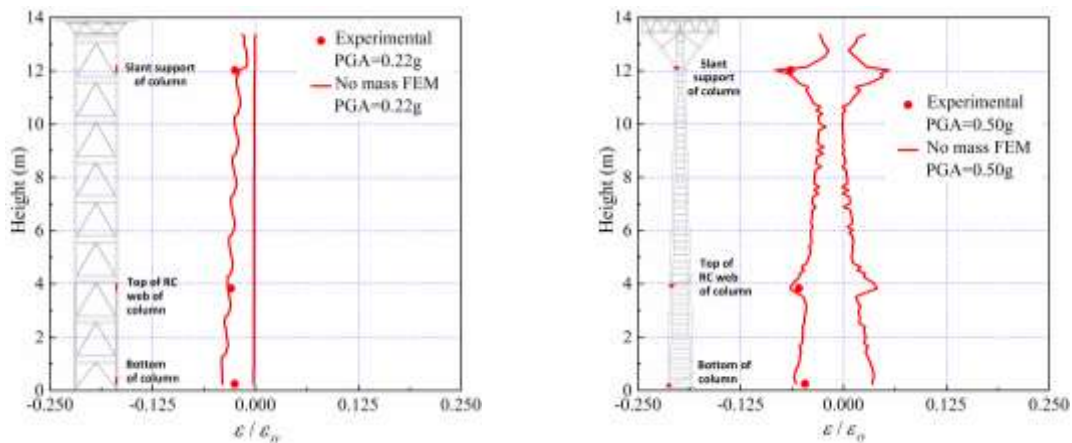
specimen, as shown in Fig. 9. In the figure, time histories of experimental result and no mass FEM are corresponding to top axis and right axis, while for full mass FEM, corresponding to bottom axis and left axis. It must be noted that some errors on the amplitude of time histories between measured and FEM, which is inevitably produced during the specimen manufacture and test procedure. However, the waveform and phase show a good results. For a more accurate assessment of the FEM, comparisons of vertical strain envelope between experimental result and FEM are presented in Fig. 10. Vertical strain envelope at the edge of circular CFST columns members along the heights are chosen in FEM. Abscissa corresponds to the ratio of measured strain dividing to the yielding strain of steel tubes. As observed, the analytical value is also in good agreement with the measured strain. Therefore, reasonable accuracy has been achieved for FEM in predicting structural seismic performance. The specimen was still in elastic stage under the maximum intensity countertop can afford in this test.



(a) Transverse excitation

(b) Longitudinal excitation

Figure 9. Comparison of displacement time histories.



(a) Transverse excitation

(b) Longitudinal excitation

Figure 10. Comparison of vertical strain envelope.

Displacement and vertical strain under longitudinal, transverse and bi-directional excitations are also compared. The maximum vertical strain comparison is illustrated in Fig. 11. As observed, vertical strain under transverse excitations is larger than under longitudinal direction at the same intensity level (PGA=0.22g), while under bi-directional excitations, it will not increase than under transverse excitations. Fig. 12 shows the maximum displacement comparisons at the top of pier. The same phenomenon could be found, displacement amplification is also not obvious. Therefore, it is unnecessary to consider the influence of bi-

directional excitations for this type bridge.

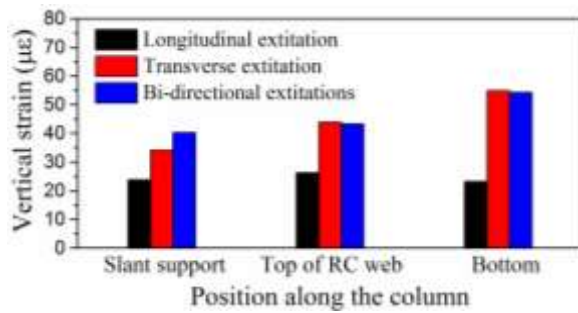


Figure 11. Vertical strain comparison.

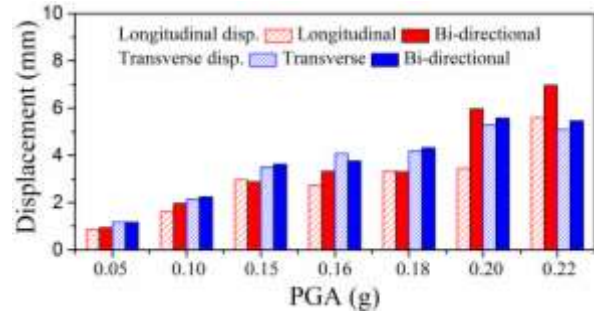


Figure 12. Displacement comparison.

Influence of ground motions

In particular, structural seismic performance need be investigated under strong ground motions. Hence, two kinds of natural records with different types, each type with three natural records, were adopted in this paper. The first is the plate boundary type of earthquakes (Type 1), having a magnitude of about 8, and the second is the inland type of earthquake (Type 2), having a magnitude of about 7-7.2 at very short distance [8]. The standard strong earthquakes of Type 1 (T111, T112, T113) and Type 2 (T211, T212, T213) in the stiff soil condition are listed in the Fig. 13. The response spectrum of these six ground motions are presented in Fig. 14. Since the restriction of test device, this work is finished by FEM analysis. According to theoretical similitude relationship, the durable time for full mass FEM is shorten by $1/\sqrt{8}$ of natural records, and the amplitude of acceleration is the same, in order to keep the strain value of FEM consistent with the real bridge. In other words, the strain value can reflect the seismic performance of real bridge.

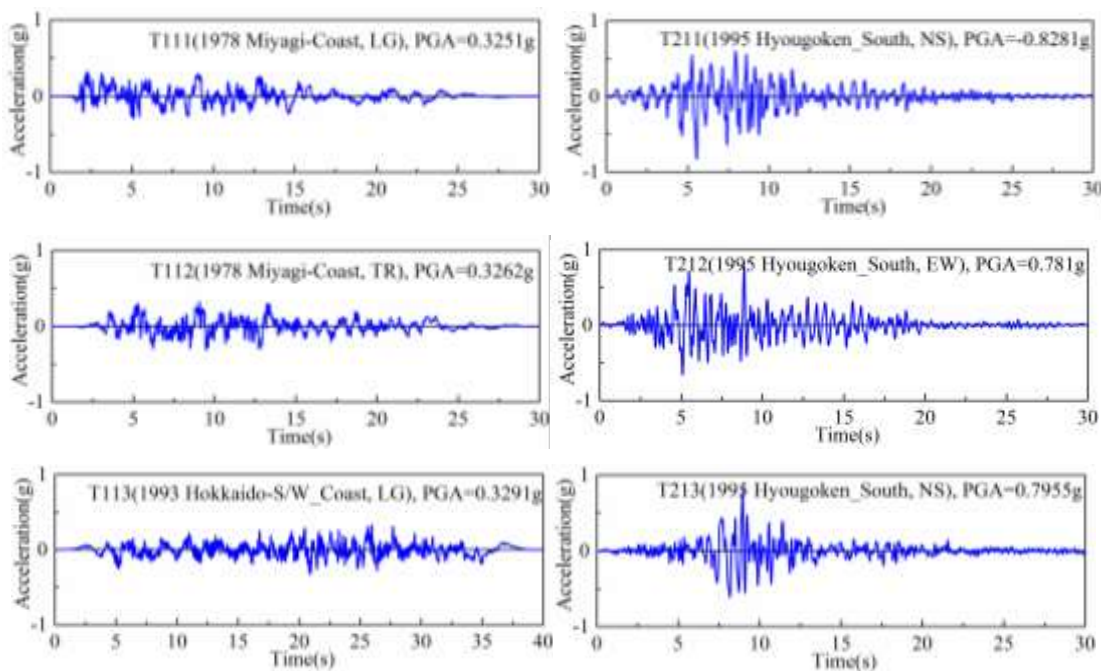


Figure 13. Time histories of natural records.

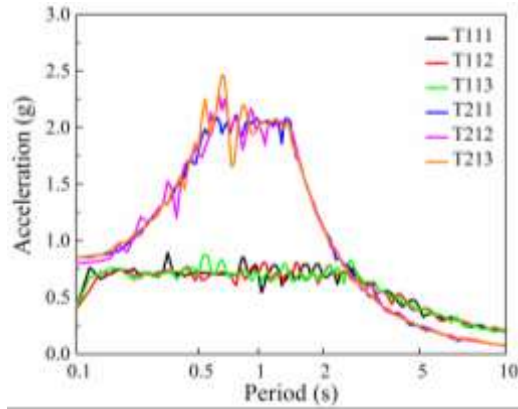


Figure 14. Response spectrum.

Fig. 15 shows the acceleration envelope of one central CFST column along the pier height. It is evident that the same calculated results will be got due to four CFST columns are symmetrical both in longitudinal and transverse directions. Results show that no matter under the longitudinal or transverse seismic excitations, acceleration subjected to Type 2 ground motions are significantly larger than subjected to Type 1 ground motions. It means that when subjected to a strong ground motions within short distance, the column can magnifies the acceleration response through remarkable oscillation on the lattice column zones, which reduces acceleration on the deck. Therefore, acceleration amplification effect on the top column does not appear for this type of pier.

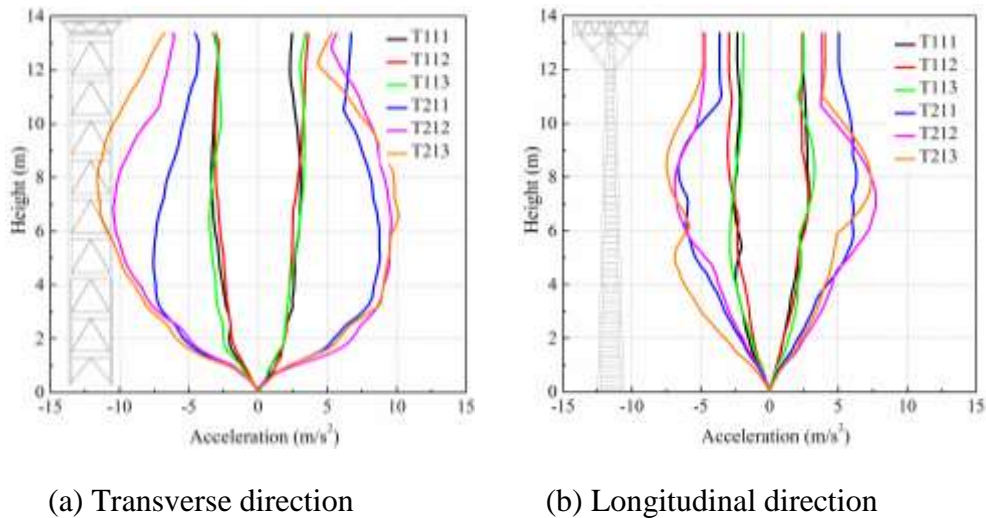
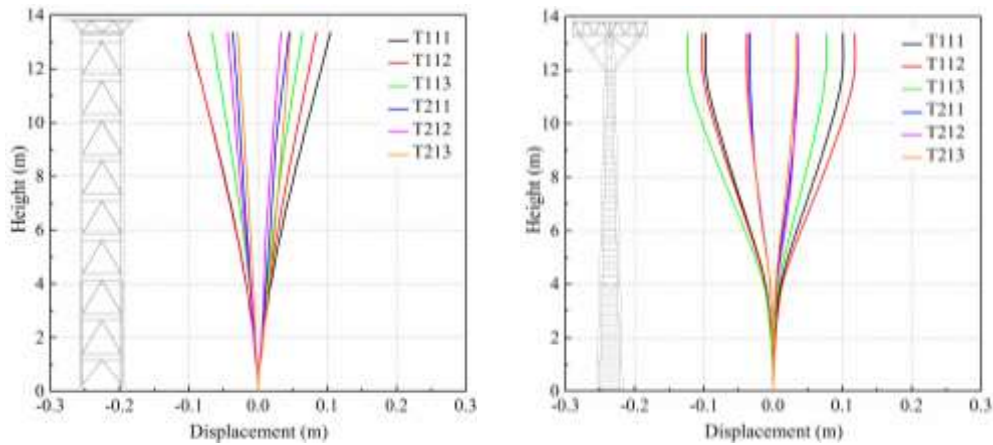


Figure 15. Acceleration envelope of pier.

While displacement envelope of the column shows opposite results, shown in Fig. 16. It can be found that both under longitudinal and transverse directional excitations, displacement subjected to Type2 ground motions are smaller than subjected to Type1 ground motions. For lack of space, Fig. 17 gives the displacement time histories comparison at the top of pier under T111 and T213 respectively. It is apparent that displacement under T111 is larger than under T213.

The maximum extreme strain of steel tube along the height are compared in Fig. 18. Abscissa is the normalized strain, if the value exceeds 1, indicating that the CFST column turn into plastic. The values under Type1 ground motions are also larger then Type2, but all the

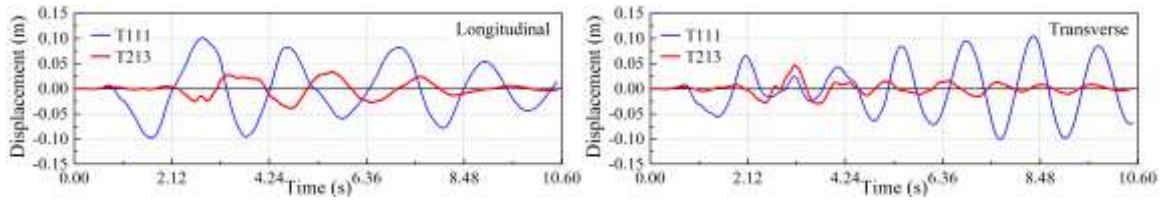
sections are remain in elastic. In transverse direction, strain envelope shows spindle-shaped, each lateral connection are relatively larger than adjacent positions, and values reduce from bottom up, thus promote seismic performance. In longitudinal direction, the stain at the position of slant support and top of RC web will be larger than other positions. The slant support shares the internal force, protect the top connection between the CFST column and girder. Subjected to strong ground motions of Type1 and Type2, the pier remain in elastic stage, it demonstrates that this innovative lightweight bridge has a favorable seismic performance.



(a) Transverse direction

(b) Longitudinal direction

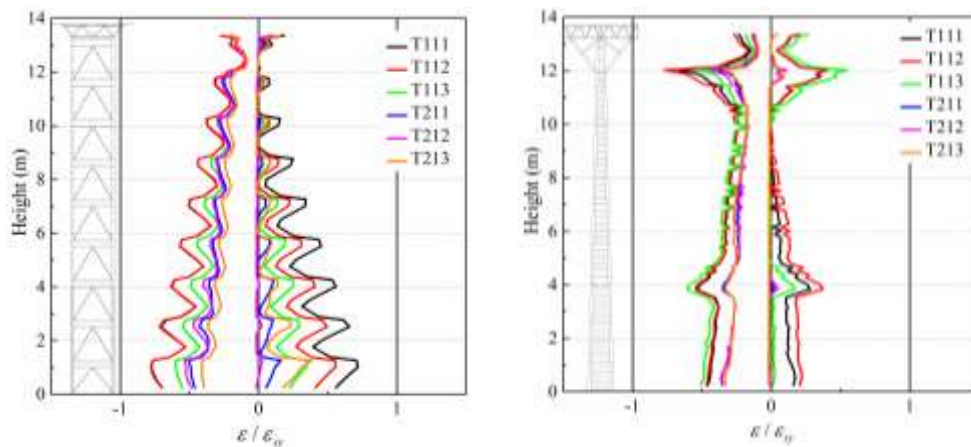
Figure 16. Displacement envelope of pier.



(a) Longitudinal direction

(b) Transverse direction

Figure 17. Time histories at the top of pier.



(a) Transverse direction

(b) Longitudinal direction

Figure 18. Normalized strain envelope at the extreme edge of steel tubes.

Conclusions

Based on test data and analytical results, summary and conclusions are made as follows:

- (1) Through white noise excitation, the identified fundamental frequency of structure is 1.45 Hz in longitudinal direction and 2.10 Hz in transverse direction. The frequency ratio between prototype and model is 1:7.47 in the first order and 1:7.69 in the second order, which are closed to theoretical frequency ratio of 1:8. According to the similitude relationship, displacement of specimen agrees well with prototype.
- (2) Under bidirectional excitations, displacement and strain are not larger than subjected to one directional seismic input. Hence, it is not necessary to consider the influence of bidirectional excitations.
- (3) The accuracy of FEM approaches is verified through comparisons of fundamental frequency, time histories of displacement and strain envelope along the column. Specimen was still in elastic stage under the maximum intensity countertop can afford in this test.
- (4) Influence of ground motions are investigated with two types of seismic records, results show that Type 1 earthquakes generate larger responses than Type 2 earthquakes in displacement and strain of column, while the acceleration subjected to Type 2 earthquakes are significantly larger than subjected to Type 1 earthquakes.
- (5) Subjected to strong ground motions of Type1 and Type2, the structure remains in elastic stage, indicating that this innovative lightweight bridge has a favorable seismic performance.

References

1. Mazzoni S, McKenna F, Fenves GL. et al. *Open System for Earthquake Engineering Simulation User Manual*. Berkeley: Pacific Earthquake Engineering Research Center. PEER, University of California, 2006.
2. Harry G. Harris, Gajanan M. Sabnis. *Structural modeling and experimental techniques*. 2nd ed. CRC Press: New York, 1999.
3. JTG/T B02-01-2008. *Guidelines for seismic design of highway bridges*. Communications Press: Beijing, 2008. In Chinese.
4. Menegotto M, Pinto PE. Method of analysis for cyclically loaded R.C. plane frames including changes in geometry and non-elastic behavior of elements under combined normal force and bending. *In: Proceedings, IABSE. Symposium on resistance and ultimate deformability of structures acted on by well defined repeated load* 1973.
5. Filippou, FC, Popov, EP, Bertero, VV. Effects of bond deterioration on hysteretic behavior of reinforced concrete joints. *Technical Report EERC 83/19, Earthquake Engineering Research Center, University of California, Berkeley* 1983.
6. Mander JB, Priestley JN, Park R. Theoretical stress-strain model for confined concrete. *Journal of Structural Engineering* 1988; **114** (8): 1804-1826.
7. Liang QQ, Fragomeni S. Nonlinear analysis of circular concrete-filled steel tubular short columns under axial loading. *Journal of Construction Steel Research* 2009; **65** (12): 2186-2196.
8. Wu QX, Yoshimura M, Takahashi K, Nakamura S, Nakamura T. Nonlinear seismic properties of the Second Saikai Bridge a concrete filled tubular (CFT) arch bridge. *Engineering Structures* 2006, 28 (2): 163-182.